Progress in Fractional Differentiation and Applications
An International Journal

http://dx.doi.org/10.18576/pfda/060105

Modeling Transient Currents in Time-of-Flight Experiments with Tempered Time-Fractional Diffusion Equations

Maria Luísa Morgado[1,*] *and Luís Filipe Morgado*[2]

[1] Center for Computational and Sthocastic Mathematics, Instituto Superior Técnico, Lisboa, Portugal and Department of Mathematics, University of Trás-os-Montes e Alto Douro, UTAD, Quinta de Prados 5001-801, Vila Real, Portugal
[2] Instituto de Telecomunicações, Lisboa, Portugal and Department of Physics, University of Trás-os-Montes e Alto Douro, UTAD, Quinta de Prados 5001-801, Vila Real, Portugal

Received: 2 Dec. 2018, Revised: 18 Jan. 2019, Accepted: 9 Feb. 2019
Published online: 1 Jan. 2020

Abstract: In the present paper, we use tempered fractional advection-diffusion equations to model the dispersive transport in disordered materials. A numerical method, on a time graded mesh, is derived to approximate the solution of such differential models. We also prove that it is convergent and stable. Two numerical examples are presented: The first, with known analytical solution, is presented to illustrate the performance of the numerical scheme; the second is used to show that such models are appropriate to model time of flight transient currents for some disordered materials.

Keywords: Tempered Caputo derivative, advection-diffusion equation, graded mesh, disordered materials, time-of-flight.

1 Introduction

Currently, Fractional Calculus, which involves the study of integral and differential operators of non-integer order, is a powerful tool in modeling various processes in science and engineering (see for example the books [1], [2], [3] and the references therein). Although it is more than three hundred years old, only in the last decades it has been intensively investigated. Since its very beginning, several renowned scientists have contributed to its development. Throughout the last three centuries, several definitions (not always equivalent) of fractional derivatives, generalising the integer-order ones, arose. We claim that the Riemann-Liouville and the Caputo derivatives are the most prevalent in the pieces of literature, mainly the last ones when application problems are considered ([2]).

Due to the features of fractional integral and differential operators, the need for numerical methods is even more evident in the fractional setting and their development poses us new challenges that did not occur when integer-order models were considered. These challenges may be resumed in two items: the computational effort because of the nonlocality of the fractional operators and the accuracy of the numerical schemes due to the singular nature of the solutions of fractional differential equations. Although numerous papers have addressed the numerical approximation of fractional differential equations in the last decades, few fully addressed the two issues.Thus, further investigation is required within this respect. Concerning the numerical approximation of time-fractional diffusion equations of the Caputo type, finite difference methods seem to be the most popular ones (see [4] and the references therein), despite the existence of other numerical methods, such as finite element methods ([5], [6]), meshless collocation methods ([7]) and collocation spectral methods ([8]). With respect to finite difference methods, the L1 formula, which we will also use here, to approximate the fractional Caputo derivative, may be the most frequently used in the literature. This formula, which consists of a direct approximation of the derivative of the solution that appears under the integral sign in the definition of the Caputo derivative, has been successfully used in numerous works, including the recent ones [9] ,[10] and [11], just to name a few.

* Corresponding author e-mail: luisam@utad.pt

The present paper handles the modeling of the transient current in time-of-flight (ToF) experiments in disordered materials. In such experiments, the transient current through a thin layer of material sandwiched between two parallel electrodes placed at $x = 0$ and $x = L$ is measured. This current is the motion, under the influence of an externally applied electric field E directed normally to the electrodes, of excess charge carriers generated by a laser or voltage pulse. Results from this experiments for disordered materials, namely organic semiconductors, usually exhibit an anomalous dispersive behavior ([12]), when the transient current $I(t)$ curve presents two regions with power-law behavior, separated by the "transit time" t_{tr}:

$$I(t) \sim \begin{cases} t^{-1+\alpha} & \text{if } t < t_{tr} \\ t^{-1-\alpha} & \text{if } t > t_{tr} \end{cases}, \quad 0 < \alpha < 1. \tag{1}$$

From experimental $I(t)$ curves, usually the t_{tr} is obtained, graphically, from the intersection of the two power-law curves, used to determine the carrier drift mobility, which is an important characteristic of materials for electronic applications. This behavior was attributed to the trapping of carriers, in localized states distributed in the mobility gap, for times τ, determined by a relaxation function with an asymptotic time dependence of the form $\sim \tau^{-\alpha}$, with non integer dispersion parameter α. Alternative physical explanations involve other mechanisms such as phonon assisted hopping conduction and percolation through conducting states. In some cases, as reported in [13], the transient current reveals two different values for the dispersive parameter: α_i for shorter times and α_f for longer times. A possible justification for this fact is based on the assumption that the energy distribution of deep traps is truncated thereby resulting in a truncated waiting time distribution ([14]).

This paper continues the investigation initiated in [15], where the following class of initial-boundary value problem is considered to describe the evolution of carrier density $u(x,t)$ (see also [16] and [14]):

$$D_t^\alpha u(x,t) = -v\frac{\partial u(x,t)}{\partial x} + D\frac{\partial^2 u(x,t)}{\partial x^2} + f(x,t),\ t \in (0,T],\ x \in (0,L), \tag{2}$$

with initial condition

$$u(x,0) = g(x), \quad x \in (0,L), \tag{3}$$

and boundary conditions

$$u(0,t) = \phi_0(t),\ \ u(L,t) = \phi_L(t), \quad t \in (0,T], \tag{4}$$

where $0 < \alpha < 1$ and the fractional derivative is of the Caputo type which, for the considered values of α, is given by ([2]):

$$D_t^\alpha y(t) = \frac{1}{\Gamma(1-\alpha)}\int_0^t (t-s)^{-\alpha} y'(s)\, ds. \tag{5}$$

Eq. (2) is suitable to describe the charge carrier number density in disordered materials, being α, the order of the fractional derivative, which can be directly related, for example, with the trapping mechanisms in localized states ([16], [17]), with smaller values of α corresponding to increasingly severe traps. When $\alpha \to 1$, $D_t^\alpha u = \dfrac{\partial u}{\partial t}$, and (2) becomes the usual advection-diffusion equation used to model the evolution of the carrier density in materials that do not exhibit a dispersive behavior. The unknown function u, referred to as the solution concentration, is the charge carrier density. $v > 0$ is the generalized average carrier velocity (related to the applied electric field E), and $D > 0$ is the generalized diffusion coefficient. We assume that g, f, ϕ_0 and ϕ_L are continuous functions in their respective domains and that v and D are constant coefficients. Although analytical solutions for fractional diffusion problems have been reported ([18],[19]), they are expressed in terms of series and are unsuitable for simulation purposes. The development of efficient numerical methods to solve such problems are highly needed if they are to be used, for example, in the interpretation and or fitting the experimental data. Some relevant steps were taken, in the study of organic semiconductor devices, for example in [20].

In [15], an implicit numerical scheme on a time graded mesh was developed to approximate the solution of the initial-boundary value problem above. A graded mesh in the time variable is used because it is known ([16]) that the solution of this type of problems exhibits a sharp behavior near the origin (which is in agreement with the fact that fractional differential equations have singularities at $t = 0$, in the sense that the derivatives of the solution may become unbounded near that point). Accordingly, to obtain reasonable accurate results it is convenient to use small step-sizes near that point. This was achieved by considering a partition of the time interval into n subintervals defined by the mesh-points:

$$t_i = \left(\frac{i}{n}\right)^r T, \tag{6}$$

where $r \geq 1$ is the so-called grading exponent. The length of each one of the intervals defined with this partition is:

$$\tau_i = t_{i+1} - t_i = \frac{(i+1)^r - i^r}{n^r} T, \quad i = 0, 1, \ldots, n-1.$$

Note that if $r=1$ we obtain a uniform mesh, i.e. a mesh where all the subintervals in the partition have the same length ($\tau_i=\tau=\frac{T}{n},\ i=0,1,\ldots,n-1$), while if $r>1$, the grid-points are more densely placed in the left-hand side of the interval $[0,T]$, as desired.
In [15], the proper choice of the grading exponent was left for future work. It is one of the aspects that need to be addressed in the present research based on the results of [10]. Moreover, the scheme presented in [15] was first order convergent in space, but the present paper develops a second order convergent method with respect to the space variable. Another contribution is that we will generalize the model (2) considering tempered Caputo derivatives instead of the Caputo ones. A preliminary version of this paper may be found in [21].

Considering the probability density function of waiting time as Lévy's distributions in the derivation of the transport equation, the usual (non-tempered) fractional Riemann-Liouville derivatives of order α arise (and consequently, the Caputo derivatives). However, because these distributions decay as $|t|^{-1-\alpha}$, first or second moments will be divergent (see [22]). Through exponentially tempering the distribution, for large waiting times, with a parameter $\lambda>0$, the probability density function will decay as $|t|^{-1-\alpha}e^{-\lambda|t|}$, finite moments are obtained, and the definition of tempered fractional derivatives arises ([23]):

$$\begin{aligned}\mathbb{D}_t^{\alpha,\lambda}\left(y(t)\right) &= e^{-\lambda t}D_t^{\alpha}\left(e^{\lambda t}y(t)\right) \\ &= \frac{e^{-\lambda t}}{\Gamma(1-\alpha)}\int_0^t \frac{1}{(t-s)^{\alpha}}\frac{d\left(e^{\lambda s}y(s)\right)}{ds}ds,\ \ 0<\alpha<1,\ \lambda\geq 0.\end{aligned} \tag{7}$$

If we consider $\lambda=0$, the definition of the usual Caputo derivative (5) is recovered.
Hence, we will consider the following model (which obviously reduces to (2)-(4) in the case where we have $\lambda=0$ and absorbing boundary conditions):

$$\mathbb{D}_t^{\alpha,\lambda}u(x,t) = -v\frac{\partial u(x,t)}{\partial x}+D\frac{\partial^2 u(x,t)}{\partial x^2}+f(x,t),\ t\in(0,T],\ x\in(0,L), \tag{8}$$

$$u(x,0)=g(x),\quad x\in(0,L), \tag{9}$$

$$u(0,t)=0,\ \ u(L,t)=0,\quad t\in(0,T], \tag{10}$$

where $\mathbb{D}_t^{\alpha,\lambda}u(x,t)$ is the tempered Caputo derivative with respect to the variable t of the function $u(x,t)$. In the modeling of dispersive transport in disordered materials, we will assume that $f(x,t)\equiv 0$. However we choose to keep this term in the above model for technical reasons. It will help build problems with known analytical solutions. Consequently, we will be able to compare our numerical results with the analytical ones.

The present paper aims to consider a general model that describes the transient currents in disordered materials and to develop an efficient numerical scheme for this kind of models which can deal with both smooth and nonsmooth solutions. To the best to our knowledge, such numerical scheme for tempered time-fractional diffusion equations has never been reported in the literature.

The paper is outlined as follows: the next section describes the numerical method to solve (8)-(10) and we prove that it is convergent and stable. In section 3, we first test the robustness of the numerical method through some numerical experiments; for an example with known analytical solution; we subsequently use it to model the transient current in ToF experiments. The last section involves the conclusion that addresses the advantages of considering this type of equations to model such processes.

2 Numerical scheme

In this section, we develop an implicit numerical method for the approximate solution of (8)-(10). First, taking (7) into account, we note that (8) can be written as

$$D_t^{\alpha}\left(e^{\lambda t}u(x,t)\right) = -v\frac{\partial\left(e^{\lambda t}u(x,t)\right)}{\partial x}+D\frac{\partial^2\left(e^{\lambda t}u(x,t)\right)}{\partial x^2}+e^{\lambda t}f(x,t).$$

If we consider the function

$$y(x,t)=e^{\lambda t}u(x,t), \tag{11}$$

and we define the solution $y(x,t)$ of problem:

$$D_t^{\alpha}y(x,t) = -v\frac{\partial y(x,t)}{\partial x}+D\frac{\partial^2 y(x,t)}{\partial x^2}+e^{\lambda t}f(x,t),\ t\in(0,T],\ x\in(0,L), \tag{12}$$

$$y(x,0)=g(x),\quad x\in(0,L), \tag{13}$$

$$y(0,t)=0,\ \ y(L,t)=0,\quad t\in(0,T], \tag{14}$$

then the solution of (8)-(10) is obtained through

$$u(x,t) = e^{-\lambda t} y(x,t).$$

Therefore, the next part presents a numerical scheme for the solution of (12)-(14). We consider a uniform mesh in the interval $[0,L]$, defined by the grid-points $x_i = ih$, $i = 0,1,\ldots,K$, where $h = \frac{L}{K}$. We also use the following second order finite difference approximations assuming that the solution possess fourth order continuous derivatives with respect to x:

$$\frac{\partial y(x_i,t)}{\partial x} \approx \frac{y(x_{i+1},t) - y(x_{i-1},t)}{2h}, \tag{15}$$

$$\frac{\partial^2 y(x_i,t)}{\partial x^2} \approx \frac{y(x_{i+1},t) - 2y(x_i,t) + y(x_{i-1},t)}{h^2}, \quad i = 1,\ldots,K-1. \tag{16}$$

For the numerical approximation of the Caputo derivative of order α on the interval $[0,T]$, we will use the non-uniform mesh (6). We also use the following approximation for the Caputo derivative (see [15]):

$$D_t^\alpha y(t_k) \approx \frac{1}{\Gamma(2-\alpha)} \sum_{j=0}^{k-1} \tau_j^{-\alpha} a_{j,k} \left(y(t_{j+1}) - y(t_j) \right) = \tilde{D}^\alpha y_k, \tag{17}$$

where

$$a_{j,k} = \left(\frac{k^r - j^r}{(j+1)^r - j^r} \right)^{1-\alpha} - \left(\frac{k^r - (j+1)^r}{(j+1)^r - j^r} \right)^{1-\alpha}, \quad j = 0,1,\ldots,k-1, \;\; k = 1,\ldots,n. \tag{18}$$

The analytical solution of this kind of problems with $f(x,t) \equiv 0$ is known (see, for example [25]) showing that a singular behavior of the solution near the origin in time can be expected. Thus, we will consider that

$$\left| \frac{\partial^\ell}{\partial t^\ell} y(x,t) \right| \leq C \left(1 + t^{\alpha-\ell} \right), \quad \ell = 0,1,2, \tag{19}$$

for some positive constant c and for all $(x,t) \in [0,L] \times (0,T]$. Hence, according to this assumption and the order of the approximation, we have (see [24]):

$$\left| D_t^\alpha y(t_k) - \tilde{D}^\alpha y_k \right| \leq C t_k^{-\alpha} n^{-\min\{2-\alpha, r\alpha\}}, \; k = 1,\ldots,n. \tag{20}$$

Using (17), we obtain:

$$D_t^\alpha y(x_i,t_l) \approx \frac{1}{\Gamma(2-\alpha)} \sum_{j=0}^{l-1} \tau_j^{-\alpha} a_{j,l} \left(y(x_i,t_{j+1}) - y(x_i,t_j) \right), \quad i = 1,\ldots,K-1, \;\; l = 1,\ldots,n, \tag{21}$$

where the coefficients $a_{j,l}$ are defined in (18). Denoting by $Y_i^l \approx y(x_i,t_l)$, $f_i^l = f(x_i,t_l)$ and substituting (15), (16) and (21) in (12), we obtain the following implicit numerical scheme:

$$\frac{1}{\Gamma(2-\alpha)} \sum_{j=0}^{l-1} \tau_j^{-\alpha} a_{j,l} \left(Y_i^{j+1} - Y_i^j \right) = -v \frac{Y_{i+1}^l - Y_{i-1}^l}{2h} + D \frac{Y_{i+1}^l - 2Y_i^l + Y_{i-1}^l}{h^2} + e^{\lambda t_l} f_i^l, \tag{22}$$
$$i = 1,\ldots,K-1, \; l = 1,\ldots,n,$$

where, according to the initial and boundary conditions (13) and (14), we have

$$Y_i^0 = g(x_i), \;\; i = 1,\ldots,K-1,$$
$$Y_0^l = 0, \;\; Y_K^l = 0, \;\; l = 1,\ldots,n.$$

Having determined the unknowns Y_i^l, $i = 1,\ldots,K-1$, $l = 1,\ldots,n$, the solution of (8)-(10) at the mesh-points will be given by:

$$u(x_i,t_l) \approx U_i^l = e^{-\lambda t_l} Y_i^l.$$

2.1 Stability of the numerical scheme

In this subsection, we prove the stability of the numerical scheme as follows:

$$T_1 Y_i^l = T_2 Y_i^{l-1} + e^{\lambda t_l} f_i^l, \;\; i = 1,\dots,K-1,\; l = 1,\dots,n, \tag{23}$$

where

$$T_1 Y_i^l = \frac{\tau_{l-1}^{-\alpha}}{\Gamma(2-\alpha)} Y_i^l + v\frac{Y_{i+1}^l - Y_{i-1}^l}{2h} - D\frac{Y_{i+1}^l - 2Y_i^l + Y_{i-1}^l}{h^2},$$

$$T_2 Y_i^{l-1} = \frac{\tau_{l-1}^{-\alpha}}{\Gamma(2-\alpha)} Y_i^{l-1} - \frac{1}{\Gamma(2-\alpha)} \sum_{j=0}^{l-2} \tau_j^{-\alpha} a_{j,l} \left(Y_i^{j+1} - Y_i^j \right).$$

We start with some auxiliary results that will be needed later.

Lemma 1.*The coefficients $a_{j,l},\; j = 0,\dots,l-2,\;\; l = 1,\dots,n$, defined by (18) satisfy:*

$$a_{j,l} > 0, \tag{24}$$

$$\sum_{j=0}^{l-2} (\tau_{j+1}^{-\alpha} a_{j+1,l} - \tau_j^{-\alpha} a_{j,l}) = -\tau_0^{-\alpha} a_{0,l} + \tau_{l-1}^{-\alpha},\; l \geq 2, \tag{25}$$

$$\tau_{j+1}^{-\alpha} a_{j+1,l} > \tau_j^{-\alpha} a_{j,l} \tag{26}$$

$$a_{0,j} \geq a_{0,l},\; j \leq l, \tag{27}$$

$$t_j^{\alpha} a_{0,j} \geq t_l^{\alpha} a_{0,l},\; j \leq l. \tag{28}$$

*Proof.*Properties (24), (25) and (26) were proved in [15].
In order to prove property (27), we consider the function

$$h(x) = x^{1-\alpha} - (x-1)^{1-\alpha},\; x \geq 1.$$

Then, since $r \geq 1$, to prove that $a_{0,j} \geq a_{0,l}$ is equivalent to prove that $h(j^r) \geq h(l^r)$, $1 \leq j < l$.
Using the mean value theorem, we have

$$h(j^r) - h(l^r) = h'(\xi)(j^r - l^r), \text{ for some } \xi \in (j^r, l^r).$$

Since

$$h'(x) = (1-\alpha)\left(x^{-\alpha} - (x-1)^{-\alpha}\right),\; x > 1,$$

the result is proved.
In order to prove (28), which is equivalent to

$$j^{r\alpha}\left(j^{r(1-\alpha)} - (j^r-1)^{1-\alpha}\right) \geq l^{r\alpha}\left(l^{r(1-\alpha)} - (l^r-1)^{1-\alpha}\right),\; j < l$$

and proceeding similarly as before, if we consider the function

$$w(x) = x^{\alpha}\left(x^{1-\alpha} - (x-1)^{1-\alpha}\right),\; x \geq 1,$$

using the mean value theorem, we have

$$w(j^r) - w(l^r) = w'(\eta)(j^r - l^r) \text{ for some } \eta \in (j^r, l^r).$$

Then, it suffices to show that $w'(x) < 0$ for $x > 1$.
In fact,

$$w'(x) = 1 - \alpha\left(1-\frac{1}{x}\right)^{1-\alpha} - (1-\alpha)\left(1-\frac{1}{x}\right)^{-\alpha} < 1 - \alpha\left(1-\frac{1}{x}\right)^{-\alpha} - (1-\alpha)\left(1-\frac{1}{x}\right)^{-\alpha} = 1 - \left(1-\frac{1}{x}\right)^{-\alpha} < 0,$$

so the desired result is obtained.

In order to prove the stability of the numerical scheme, we assume that the initial data has error ε_i^0, i.e. we assume that $\tilde{g}(x_i) = g(x_i) + \varepsilon_i^0$, $i = 1,2,\ldots,K-1$, and let Y_i^l and $\tilde{Y}_i^l$ be the solutions of (23) corresponding to the initial data g and $\tilde{g}$, respectively. Defining $\varepsilon_i^l = Y_i^l - \tilde{Y}_i^l$, we have

$$T_1\varepsilon_i^l = T_2\varepsilon_i^{l-1}, \quad i = 1,2,\ldots,K-1,\ l = 1,2,\ldots,n.$$

Setting $\left\|E^l\right\|_\infty = \max_{1\le i\le K-1}\left|\varepsilon_i^l\right|$, we subsequently prove, using mathematical induction, that

$$\left\|E^l\right\|_\infty \le \left\|E^0\right\|_\infty$$

is satisfied for all $l = 1,2,\ldots,n$.
For $l = 1$, let $p \in \mathbb{N}$ be such that $\left\|E^1\right\|_\infty = \max_{1\le i\le K-1}\left|\varepsilon_i^1\right| = \left|\varepsilon_p^1\right|$. Then,

$$\begin{aligned}\frac{\tau_0^{-\alpha}}{\Gamma(2-\alpha)}\left\|E^1\right\|_\infty &= \frac{\tau_0^{-\alpha}}{\Gamma(2-\alpha)}\left|\varepsilon_p^1\right| = \frac{\tau_0^{-\alpha}}{\Gamma(2-\alpha)}\left|\varepsilon_p^1\right| + \frac{2D}{h^2}\left|\varepsilon_p^1\right| - \frac{2D}{h^2}\left|\varepsilon_p^1\right| + \frac{2D}{h^2}\left|\varepsilon_p^1\right| \\ &= \frac{\tau_0^{-\alpha}}{\Gamma(2-\alpha)}\left|\varepsilon_p^1\right| + \frac{2D}{h^2}\left|\varepsilon_p^1\right| - \left(\frac{D}{h^2} - \frac{v}{2h}\right)\left|\varepsilon_p^1\right| - \left(\frac{D}{h^2} + \frac{v}{2h}\right)\left|\varepsilon_p^1\right|\end{aligned}$$

If $h < \dfrac{2D}{v}$, then $\dfrac{2D - vh}{2h^2} > 0$. Therefore,

$$\begin{aligned}\frac{\tau_0^{-\alpha}}{\Gamma(2-\alpha)}\left\|E^1\right\|_\infty &\le \frac{\tau_0^{-\alpha}}{\Gamma(2-\alpha)}\left|\varepsilon_p^1\right| + \frac{2D}{h^2}\left|\varepsilon_p^1\right| - \left(\frac{D}{h^2} - \frac{v}{2h}\right)\left|\varepsilon_{p+1}^1\right| - \left(\frac{D}{h^2} + \frac{v}{2h}\right)\left|\varepsilon_{p-1}^1\right| \\ &\le \left|\frac{\tau_0^{-\alpha}}{\Gamma(2-\alpha)}\varepsilon_p^1 + v\frac{\varepsilon_{p+1}^1 - \varepsilon_{p-1}^1}{2h} - D\frac{\varepsilon_{p+1}^1 - 2\varepsilon_p^1 + \varepsilon_{p-1}^1}{h^2}\right| \\ &= \left|T_1\varepsilon_p^1\right| = \left|T_2\varepsilon_p^0\right| = \left|\frac{\tau_0^{-\alpha}}{\Gamma(2-\alpha)}\varepsilon_p^0\right| \le \frac{\tau_0^{-\alpha}}{\Gamma(2-\alpha)}\left\|E^0\right\|_\infty,\end{aligned}$$

and then if follows that $\left\|E^1\right\|_\infty \le \left\|E^0\right\|_\infty$.
Now, let us assume that $\left\|E^j\right\|_\infty \le \left\|E^0\right\|_\infty$, $j = 1,\ldots,l-1$, and $p \in \mathbb{N}$ is such that $\left\|E^l\right\|_\infty = \left|\varepsilon_p^l\right|$. Hence following the same steps as above,

$$\begin{aligned}\frac{\tau_{l-1}^{-\alpha}}{\Gamma(2-\alpha)}\left\|E^l\right\|_\infty &= \frac{\tau_{l-1}^{-\alpha}}{\Gamma(2-\alpha)}\left|\varepsilon_p^l\right| \le \left|T_1\varepsilon_p^l\right| = \left|T_2\varepsilon_p^{l-1}\right| \\ &= \left|\frac{\tau_{l-1}^{-\alpha}}{\Gamma(2-\alpha)}\varepsilon_p^{l-1} - \frac{1}{\Gamma(2-\alpha)}\sum_{j=0}^{l-2}\tau_j^{-\alpha}a_{j,l}\left(\varepsilon_p^{j+1} - \varepsilon_p^j\right)\right| \\ &= \frac{1}{\Gamma(2-\alpha)}\left|\tau_0^{-\alpha}a_{0,l}\varepsilon_p^0 + \sum_{j=0}^{l-2}\left(\tau_{j+1}^{-\alpha}a_{j+1,l} - \tau_j^{-\alpha}a_{j,l}\right)\varepsilon_p^{j+1}\right|.\end{aligned}$$

Using (26), the induction hypothesis and (25), it follows that:

$$\begin{aligned}\frac{\tau_{l-1}^{-\alpha}}{\Gamma(2-\alpha)}\left\|E^l\right\|_\infty &\le \frac{1}{\Gamma(2-\alpha)}\left(\tau_0^{-\alpha}a_{0,l}\left|\varepsilon_p^0\right| + \sum_{j=0}^{l-2}\left(\tau_{j+1}^{-\alpha}a_{j+1,l} - \tau_j^{-\alpha}a_{j,l}\right)\left|\varepsilon_p^{j+1}\right|\right) \\ &\le \frac{\left\|E^0\right\|_\infty}{\Gamma(2-\alpha)}\left(\tau_0^{-\alpha}a_{0,l} + \sum_{j=0}^{l-2}\left(\tau_{j+1}^{-\alpha}a_{j+1,l} - \tau_j^{-\alpha}a_{j,l}\right)\right) \\ &= \frac{\left\|E^0\right\|_\infty}{\Gamma(2-\alpha)}\tau_{l-1}^{\alpha}.\end{aligned}$$

We can conclude that $\left\|E^l\right\|_\infty \le \left\|E^0\right\|_\infty$, $l = 1,2,\ldots,n$. Thus, the following result is proved.

Theorem 1. *If $h < \dfrac{2D}{v}$, the numerical scheme (23) is stable.*

2.2 Convergence of the numerical scheme

In order to prove the convergence order of the numerical scheme, let us first note that taking into account (15), (16), (20) and (21) , the solution of (12)-(14) satisfies:

$$\frac{1}{\Gamma(2-\alpha)}\sum_{j=0}^{l-1}\tau_j^{-\alpha}a_{j,l}\left(y(x_i,t_{j+1})-y(x_i,t_j)\right)=-v\frac{y(x_{i+1},t_l)-y(x_{i-1},t_l)}{2h}$$
$$+D\frac{y(x_{i+1},t_l)-2y(x_i,t_l)+y(x_{i-1},t_l)}{h^2}+e^{\lambda t_l}f_i^l+R_i^l,\ \ i=1,\ldots,K-1,\ l=1,\ldots,n,$$

where $\left\|R^l\right\|_\infty=\max_{1\le i\le K-1}\left|R_i^l\right|\le C_1(t_l^{-\alpha}n^\beta+h^2)$, being $\beta=-\min\{2-\alpha,r\alpha\}$ and C_1 a positive constant not depending on n or h. Define the error at every point of the mesh by

$$e_i^l=y(x_i,t_l)-Y_i^l,\ \ i=1,\ldots,K-1,\ l=1,\ldots,n,$$

and $\mathbf{e}^l=(e_1^l\ \ e_2^l\ \ldots\ e_{K-1}^l)^T$. Obviously $\mathbf{e}^0=(0\ \ 0\ \ldots\ 0)^T$, and

$$T_1e_i^l=T_2e_{i-1}^l+R_i^l,\ \ i=\ldots,K-1,\ \ l=1,\ldots,n.$$

We first prove the following result:

Lemma 2.*Assume that $h<\frac{2D}{v}$. There exists a positive constant C_1 not depending on n and h such that:*

$$\left\|\mathbf{e}^l\right\|_\infty\le\frac{C_1(t_l^{-\alpha}n^\beta+h^2)}{\frac{1}{\Gamma(2-\alpha)}\left(\tau_{l-1}^{-\alpha}-\sum_{j=0}^{l-2}\left(\tau_{j+1}^{-\alpha}a_{j+1,l}-\tau_j^{-\alpha}a_{j,l}\right)\right)},\ \ l=1,2,\ldots,n. \tag{29}$$

*Proof.*We use mathematical induction to prove (29). Similarly to the proof of stability, for $l=1$, let $p\in\mathbb{N}$ be such that $\left\|\mathbf{e}^1\right\|_\infty=\max_{1\le i\le K-1}\left|e_i^1\right|=\left|e_p^1\right|$. Then,

$$\frac{\tau_0^{-\alpha}}{\Gamma(2-\alpha)}\left\|\mathbf{e}^1\right\|_\infty=\frac{\tau_0^{-\alpha}}{\Gamma(2-\alpha)}\left|e_p^1\right|\le\left|T_1e_p^1\right|=\left|T_2e_p^0+R_p^1\right|=\left|R_p^1\right|\le\left\|R^1\right\|_\infty\le C_1(t_1^{-\alpha}n^\beta+h^2),$$

and then (29) is satisfied for $l=1$. Assume now that

$$\left\|\mathbf{e}^j\right\|_\infty\le\frac{C_1(t_j^{-\alpha}n^\beta+h^2)}{\frac{1}{\Gamma(2-\alpha)}\left(\tau_{j-1}^{-\alpha}-\sum_{m=0}^{j-2}\left(\tau_{m+1}^{-\alpha}a_{m+1,j}-\tau_m^{-\alpha}a_{m,j}\right)\right)},\ \ j=1,2,\ldots,l-1,$$

and that $p\in\mathbb{N}$ is such that $\left\|\mathbf{e}^l\right\|_\infty=\left|e_p^l\right|$. Hence,

$$\frac{\tau_{l-1}^{-\alpha}}{\Gamma(2-\alpha)}\left\|\mathbf{e}^l\right\|_\infty=\frac{\tau_{l-1}^{-\alpha}}{\Gamma(2-\alpha)}\left|e_p^l\right|\le\left|T_1e_p^l\right|=\left|T_2e_p^{l-1}+R_p^l\right|$$
$$=\left|\frac{\tau_{l-1}^{-\alpha}}{\Gamma(2-\alpha)}e_p^{l-1}-\frac{1}{\Gamma(2-\alpha)}\sum_{j=0}^{l-2}\tau_j^{-\alpha}a_{j,l}\left(e_p^{j+1}-e_p^j\right)+R_p^l\right|$$
$$=\left|\frac{1}{\Gamma(2-\alpha)}\sum_{j=0}^{l-2}\left(\tau_{j+1}^{-\alpha}a_{j+1,l}-\tau_j^{-\alpha}a_{j,l}\right)e_p^{j+1}+R_p^l\right|$$
$$\le\frac{1}{\Gamma(2-\alpha)}\sum_{j=0}^{l-2}\left(\tau_{j+1}^{-\alpha}a_{j+1,l}-\tau_j^{-\alpha}a_{j,l}\right)\left\|\mathbf{e}^{j+1}\right\|_\infty+\left\|R^l\right\|_\infty.$$

Using the induction hypothesis, properties (27) and (28) in Lemma 1, and noting that

$$B_j=\tau_{j-1}^{-\alpha}-\sum_{m=0}^{j-2}\left(\tau_{m+1}^{-\alpha}a_{m+1,j}-\tau_m^{-\alpha}a_{m,j}\right)=\tau_0^{-\alpha}a_{0,j},$$

we obtain

$$\frac{\tau_{l-1}^{-\alpha}}{\Gamma(2-\alpha)}\left\|\mathbf{e}^l\right\|_\infty \le \frac{1}{\Gamma(2-\alpha)}\sum_{j=0}^{l-2}\left(\tau_{j+1}^{-\alpha}a_{j+1,l}-\tau_j^{-\alpha}a_{j,l}\right)\frac{C_1(t_{j+1}^{-\alpha}n^\beta+h^2)}{\frac{1}{\Gamma(2-\alpha)}\left(\tau_j^{-\alpha}-\sum_{m=0}^{j-1}\left(\tau_{m+1}^{-\alpha}a_{m+1,j+1}-\tau_m^{-\alpha}a_{m,j+1}\right)\right)}$$

$$+\ C_1(t_l^{-\alpha}n^\beta+h^2)$$

$$=\sum_{j=0}^{l-2}\left(\tau_{j+1}^{-\alpha}a_{j+1,l}-\tau_j^{-\alpha}a_{j,l}\right)\frac{C_1(t_{j+1}^{-\alpha}n^\beta+h^2)}{\tau_0^{-\alpha}a_{0,j+1}}+C_1(t_l^{-\alpha}n^\beta+h^2)$$

$$\le\sum_{j=0}^{l-2}\left(\tau_{j+1}^{-\alpha}a_{j+1,l}-\tau_j^{-\alpha}a_{j,l}\right)\frac{C_1(t_l^{-\alpha}n^\beta+h^2)}{\tau_0^{-\alpha}a_{0,l}}+C_1(t_l^{-\alpha}n^\beta+h^2)$$

$$=\frac{C_1(t_l^{-\alpha}n^\beta+h^2)\tau_{l-1}^{-\alpha}}{\left(\tau_{l-1}^{-\alpha}-\sum_{m=0}^{l-2}\left(\tau_{m+1}^{-\alpha}a_{m+1,l}-\tau_m^{-\alpha}a_{m,l}\right)\right)}.$$

Hence, the result is proved.

The result about the convergence order is presented in the next theorem:

Theorem 2.*There exists a positive constant C not depending on n and h, such that*

$$\left\|\mathbf{e}^l\right\|_\infty \le C(n^\beta+h^2),\ \ l=1,\dots,n,$$

where $\beta=-\min\{2-\alpha,r\alpha\}$.

*Proof.*First note that from Lemma 1,

$$\tau_{l-1}^{-\alpha}-\sum_{j=0}^{l-2}\left(\tau_{j+1}^{-\alpha}a_{j+1,l}-\tau_j^{-\alpha}a_{j,l}\right)=\tau_0^{-\alpha}a_{0,l}=\tau_0^{-\alpha}\left((l^r)^{1-\alpha}-(l^r-1)^{1-\alpha}\right).$$

Since

$$\lim_{l\to\infty}\frac{(l^r)^{-\alpha}}{(l^r)^{1-\alpha}-(l^r-1)^{1-\alpha}}=\lim_{\eta\to\infty}\frac{\eta^{-\alpha}}{\eta^{1-\alpha}-(\eta-1)^{1-\alpha}}=\frac{1}{1-\alpha},$$

there must exist a positive constant C_2, not depending on n and h, such that (29) becomes

$$\left\|\mathbf{e}^l\right\|_\infty \le \frac{C_1C_2(t_l^{-\alpha}n^\beta+h^2)}{\frac{1}{\Gamma(2-\alpha)}(l^r)^{-\alpha}\tau_0^{-\alpha}}=\frac{C_1C_2(t_l^{-\alpha}n^\beta+h^2)}{\frac{1}{\Gamma(2-\alpha)}t_l^{-\alpha}}\le C_3(n^\beta+t_l^\alpha h^2)\le C(n^\beta+h^2).$$

*Remark.*Using this graded mesh, and taking into account this last Theorem, we see that the time accuracy of $(2-\alpha)$ is recovered in the case of nonsmooth enough solutions, if we choose the grading exponent to be $r=\frac{2-\alpha}{\alpha}$.

3 Numerical results

To illustrate the efficiency of the proposed numerical method, we first consider an example with a known analytical solution. By taking $v=D=1$, $T=L=1$ and $g(x)=0$ in (8)-(10), the function $f(x,t)$ is defined in such a way that the exact solution is given by $u(x,t)=e^{-\lambda t}t^\alpha x(1-x)$. We have only been be concerned with the improvement of the time accuracy, which is achieved with the graded time mesh. Thus, we have fixed the small space stepsize $h=10^{-3}$ in our numerical experiments.
Table 1 presents, for this example with $\alpha=0.5$ and $\lambda=1$, the values of the maximum of the absolute errors at the discretization points:

$$E=\max_{i,j}\left|u(x_i,t_j)-U_i^j\right|,$$

as well as experimental time convergence orders (EOC). The results reveal that the time convergence order increases using a graded mesh with grading exponent $r=3$. To illustrate that the method can be also applied to usual (non-tempered) fractional differential equations, we present in Table 2 the obtained numerical values in the case where $\alpha=0.25$ and

Table 1: Absolute errors and experimental time convergence order for the first example with $\alpha = 0.5$ and $\lambda = 1$.

	$r=1$		$r=3$	
n	E	EOC	E	EOC
10	4.11×10^{-3}	-	1.48×10^{-3}	-
20	3.92×10^{-3}	0.07	7.57×10^{-4}	0.97
40	3.54×10^{-3}	0.15	3.38×10^{-4}	1.16
80	3.05×10^{-3}	0.21	1.39×10^{-4}	1.29
160	2.54×10^{-3}	0.26	5.40×10^{-5}	1.36
320	2.05×10^{-3}	0.31	2.03×10^{-5}	1.41

Table 2: Absolute errors and experimental time convergence order for the first example with $\alpha = 0.25$ and $\lambda = 0$.

	$r=1$		$r=7$	
n	E	EOC	E	EOC
5	3.94×10^{-3}	-	4.09×10^{-3}	-
10	3.90×10^{-3}		2.47×10^{-3}	0.72
20	3.79×10^{-3}	0.04	1.12×10^{-3}	1.14
40	3.66×10^{-3}	0.05	4.33×10^{-4}	1.37
80	3.52×10^{-3}	0.06	1.53×10^{-4}	1.50
160	3.36×10^{-3}	0.07	5.10×10^{-5}	1.59

$\lambda = 0$. The results indicate that, also for non-tempered Caputo models, the experimental convergence orders improve using a graded mesh with graded exponent $\frac{2-\alpha}{\alpha}$.

Next, we consider the problem we address here, i.e. modeling transient currents in ToF experiments. The total measured current $I(t)$, produced by the extraction of carriers from the space between the electrodes, placed at $x = 0$ and $x = L$, is given ([16]) by the space average of the current density $j(x,t)$

$$I(t) = \frac{1}{L}\int_0^L j(x',t)dx', \tag{30}$$

and since

$$j(x',t) = -\frac{d}{dt}\int_0^{x'} qu(x,t)dx, \tag{31}$$

where q is the carrier electrical charge, we get

$$\frac{I(t)}{q} = -\frac{d}{dt}\int_0^L (L-x)u(x,t)dx, \tag{32}$$

being $u(x,t)$ the solution of problem (8)-(10) with $f(x,t) \equiv 0$.

We use a set of data from [13] corresponding to measured currents in amorphous boron (β-rhombohedral boron), presented in Figure 1 (symbols). As mentioned above, these data do not allow a description based on a single dispersive parameter. Considering the model with tempered fractional derivatives, we obtain the approximate curve (solid line) that fits quite well to the data with $\alpha = 0.66$ and $\lambda = 1.0t_T^{-1}$. In the simulation, we consider that the initial carrier number density is Gaussian distributed around $x = 0.2L$, namely $g(x) \propto \exp(-2\times10^3(x-0.2L)^2)$, with $v = 0.38/L(t_T^{-\alpha})$, $D = 2.7\times10^{-3}/L^2(t_T^{-\alpha})$ and $r = 2$.

It should be mentioned that a good fit could not have been obtained with model (2)-(4) with a single value for the dispersive parameter α, as explained in the Introduction. Hence, the proposed model is more flexible in the sense that the materials, which could be accurately described with the model in [15], continue to be reproduced using model (8)-(10) with $\lambda = 0$. For other materials, as the β-rhombohedral boron, we need to use model (8)-(10) and adjust not only the dispersive parameter α, but also the tempered parameter λ.

4 Conclusion

We have used tempered fractional diffusion-advection equations to model transient currents in ToF experiments in disordered materials. A numerical scheme which is stable and $O(n^{-2-\alpha}+h^2)$ accurate, has been developed. The

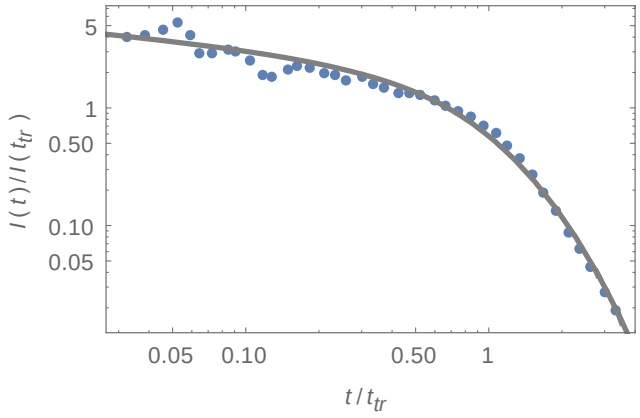

Fig. 1: Transient current for amorphous boron (β-rhombohedral boron). Dots: experimental data from [13]; Solid line: fitted curve from tempered fractional derivatives model with $\alpha = 0.66$ and $\lambda = 1.0t_T^{-1}$.

numerical results show that it is insufficient for some materials to consider fractional differential models as (2). In addition, the models improve using tempered fractional derivatives instead of the usual ones.

Acknowledgments

First author is supported by Portuguese funds through CEMAT - Center for Computacional and Sthocastic Mathematics, and the Portuguese Foundation for Science and Technology (FCT-Fundação para a Ciência e a Tecnologia), within project UID/Multi/04621/2013. Second author acknowledges financial support from Portuguese Foundation for Science and Technology (FCT), under the contract PEst-OE/EEI/LA0008/2013.

References

[1] D. Baleanu, K. Diethelm, E. Scalas and J. J. Trujillo, *Fractional calculus models and numerical methods*, Series on Complexity Nonlinearity and Chaos, World Scientific, Boston, 2012.
[2] Kai Diethelm, *The analysis of fractional differential equations: An application-oriented exposition using differential operators of Caputo type*, Springer, 2010.
[3] S. G. Samko, A. A. Kilbas and O. I. Marichev, *Fractional Integrals and Derivatives: Theory and Applications*, Gordon and Breach, Yverdon, 1993.
[4] Changpin Li, Fanhai Zeng, *Numerical methods for fractional Calculus*, Chapman & Hall/CRC Numerical Analysis and Scientific Computing Series, 2015.
[5] H.G. Sun, W. Chen and K.Y. Sze, A semi-discrete finite element method for a class of time-fractional diffusion equations *Phil. Trans. R. Soc. A* 371, 20120268. (doi:10.1098/rsta. 2012.0268) (2013).
[6] Jiang YingJun and MA JingTang, Moving finite element methods for time fractional partial differential equations, *Science China Mathematics* 56, 1287–1300 (2013).
[7] Y.T. Gu and P. Zhuang, Anomalous sub-diffusion equations by the meshless collocation method, *Australian Journal of Mechanical Engineering* 10, 1–8 (2012).
[8] H. Fenghui, A time-space collocation spectral approximation for a class of time fractional differential equations, *International Journal of Differential Equations*, Article ID 495202 (2012) doi:10.1155/2012/495202 (2012).
[9] B. Jin, R. Lazarov, and Z. Zhou, An analysis of the L1 scheme for the subdiffusion equation with nonsmooth data, *IMA J. Numer. Anal.*, 36, 197–221 (2016).
[10] Martin Stynes, Eugene O'Riordan, and José Luis Gracia, Error analysis of a finite difference method on graded meshes for a time-fractional diffusion equation, *SIAM J. Numer. Anal.*, 55 **2**, 1057–1079 (2017).
[11] Yubin Yan, Monzorul Khan, and Neville J. Ford, An analysis of the modified L1 scheme for time-fractional partial differential equations with nonsmooth data, *SIAM Journal on Numerical Analysis*, 56, **1**, 210–227 (2018).
[12] Scher, H. and Montroll, E., Anomalous transit-time dispersion in amorphous solids, *Phys. Rev. B* **12**, 2455–2477 (1975).
[13] M. Takeda, K. Kimura and K. Murayama, Transient Photocurrent Studies on Amorphous and β-Rhombohedral Boron, *J. of Solid State Chemistry* **133** 201 (1997).

[14] V. V. Uchaikin and R. T. Sibatov, *Fractional Kinetics in Solids: Anomalous Charge Transport in Semiconductors, Dielectrics and Nanosystems*, World Scientific, 2012.
[15] L. F. Morgado and M. L. Morgado, Numerical modelling transient current in the time-of-flight experiment with time-fractional advection-diffusion equations, *Journal of Mathematical Chemistry* 53 **3**, 958–973 (2015).
[16] B. W. Philippa, R. D. White and R. E. Robson, Analytic solution of the fractional advection-diffusion equation for the time-of-flight experiment in a finite geometry, *Phys. Rev. E* **84**, 041138 (2011).
[17] Peter W. Stokes, Bronson Philippa, Wayne Read and Ronald D. White, Efficient numerical solution of the time fractional diffusion equation by mapping from its Brownian counterpart, *Journal of Computational Physics*, 282, 334–344 (2015).
[18] R. Metzler, J. Klafter,Boundary value problems for fractional diffusion equations, *Physica A: Statistical Mechanics and its Applications*, 278, 107–125 (2000).
[19] O. P. Agrawal,Solution for a Fractional Diffusion-Wave Equation Defined in a Bounded Domain, *Nonlinear Dynamics*, 29, 145–155 (2002).
[20] K.Y. Choo and S.V. Muniandy and K.L. Woon and M.T. Gan and D.S. Ong,Modeling anomalous charge carrier transport in disordered organic semiconductors using the fractional drift-diffusion equation, *Organic Electronics*, 41, 157–165 (2017).
[21] M. L. Morgado and L. F. Morgado, Modeling Transient Currents in Time-of-Flight Experiments with Tempered Time-Fractional Diffusion Equations, arXiv:1811.01497 [math.NA] (2018).
[22] Uchaikin, V. V. and Zolotarev, V. M., *Chance and stability*, Stable distributions and their applications, VSP, Utrecht, The Netherlands, 1999.
[23] B. Baeumer and M. M. Meerschaert, Tempered stable Lévy motion and transient super-diffusion, *J. Comput. Appl. Math.* 233 **10**, 2438–2448 (2010).
[24] N. Kopteva, Error analysis of the L1 method on graded and uniform meshes for a fractionalderivative problem in two and three dimensions, *Mathematics of Computation*, 88, 1–20 (2017).
[25] F. Huang and F. Liu, The time fractional diffusion and advection-dispersion equation, *The ANZIAM Journal* 46 **03**, 317–330 (2005).